Molecular Modeling Studies of Aldose Reductase Inhibitors

Yong S. Lee,*,† Robert Pearlstein,‡ and Peter F. Kador†

National Eye Institute and Division of Computer Research and Technology, National Institutes of Health, Bethesda, Maryland 20892

Received July 9, 1993•

Molecular modeling studies using the AM1 quantum chemical method and a torsional fitting method have been conducted on a series of aldose reductase inhibitors (ARIs) possessing an ionizable group and/or functional group susceptible to nucleophilic attack with the aim of defining the spatial position of ARI pharmacophores. AM1 quantum chemical calculations were conducted on ARIs possessing only an ionizable group to obtain their optimized geometries. These optimized structures were then superimposed on the model compound spirofluorene-9,5′-imidazolidine-2′,4′-dione (**17**). This superposition study suggests that a negative charge center residing in the vicinity of the 2′-oxygen of the imidazolidine-2′,4′-dione ring participates in the binding interactions. In addition, the optimized geometries of ARIs possessing both an ionizable group and an electronegative functional group were superimposed on spirofluorene-9,5′-imidazolidine-2′,4′-dione (**17**). The latter results also suggest the presence of a region where nucleophilic substitution can occur.

Introduction

Aldose reductase has been linked to the accumulation of polyols which results in diabetes-associated structural and/or functional changes of peripheral nerves, lens, retina, cornea, iris, and kidney.[1-3] Observations that these changes can be ameliorated through inhibition of aldose reductase has spurred great interest in the development of aldose reductase inhibitors (ARIs) since these compounds appear to provide a pharmacologically direct treatment for diabetic complications that is independent of the control of blood sugar levels.

From the initial findings that long chain fatty acids inhibit aldose reductase, a variety of structurally diverse compounds have been observed to inhibit this enzyme. These include compounds containing the chromone, flavone, quinoline, coumarin, xanthone, 11-oxo-11*H*-pyrido[2,1-*b*]quinazoline, naphthalene, 4-oxo-3*H*-phthalazine, 2,4-dioxo-1,2,3,4-tetrahydroquinazoline, 3-thioxo-2*H*-1,4-benzoxazine, or rhodanine ring system.[1-6] Several of these compounds have progressed to the clinical level. These compounds can be divided into two general groups of ARIs, those containing a carboxylic acid moiety (Figure 1) and those containing rigid spirohydantoins or related ring systems (Figure 2).

Despite the apparent structural diversity of ARIs, certain common electronic and steric features have become apparent through computer modeling, molecular orbital calculations, and known structure–activity relationships (SAR). Kador et al.[1,4-6] have shown that the structural requirements for activity consist of a generally planar structure with two hydrophobic (aromatic) regions and a common region which is susceptible to charge-transfer interactions. On the basis of this observation, they proposed that the inhibitor binding site of aldose reductase (e.g., rat lens) possesses a hydrophobic (lipophilic) region and a region at which reversible charge-transfer (nucleophilic substitution) can occur. The existence of a nucleophilic residue in the inhibitor binding site has been demonstrated using the protein-modifying agents benzenesulfonyl fluoride and 2-bromo-4-nitroacetophenone. A series of affinity labels based on the structures of **12**, alrestatin (**1**), and sorbinil (**9**) have also been utilized to define the spatial requirements of the nucleophilic residue(s) within the inhibitor site.[7-9] Kinetic studies[3-6] indicate that ARIs reversibly inhibit the enzyme by interacting at a site different from either the substrate or the NADPH-binding site. Competition studies using different ARIs also suggest that ARIs interact at a single common site on the enzyme.[3]

Most ARIs to date contain either an ionizable group (e.g., carboxylic acid) or a hydantoin ring possessing an electronegative functional group.[10-13] Thus, we have conducted molecular modeling studies on ARIs possessing

	Structure	Name	Developer
1	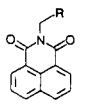	Alrestatin AY 22,284	Ayerst, USA
2		Isodibut	Inst. Endocrin. Metab. Kiev, USSR
3	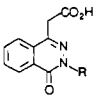	Ponalrestat Statil ICI 128426	ICI, England
4		Zopolrestat CP 73,850	Pfizer, USA
5	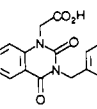	FK 366 FR 74366	Fujisawa, Japan
6	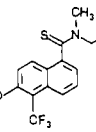	Aldredase Tolrestat AY 27,773	Wyeth-Ayerst, USA
7		Epalrestat ONO 2235	Ono, Japan
8	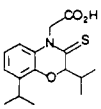	AD 5467	Takeda, Japan

Figure 1. Clinically tested aldose reductase inhibitors containing carboxylic acids.

* Address correspondence to: Yong S. Lee, Bldg 10 Rm 10B-13, LOT/NEI/NIH, 9000 Rockville Pike, Bethesda, MD 20892. Telephone (301) 496-0589. FAX (301) 402-2399.
† National Eye Institute.
‡ Division of Computer Research and Technology.
• Abstract published in *Advance ACS Abstracts*, January 15, 1994.

0022-2623/94/1837-0787$04.50/0

	Structure	R	R'	Name	Developer
9	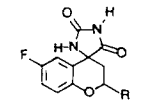	H		Sorbinil CP 45,634	Pfizer, USA
10		CH_3		M 79175 Methosorbinil E 0722	Eisai, Japan Dispersa, Switzerland
11		O C-NH_2		SNK 860	Samwa, Japan
12	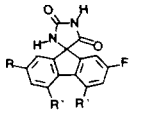	H	H	Alconil Al 1567	Alcon, USA
13		F	H	Al 1576 Imirestat HOE 843	Alcon, USA Hoechst, Germany
14		F	OCH_3	Al 4114	Alcon, USA
15	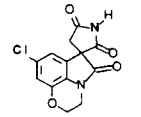			ADN 138	Kyorin, Japan
16	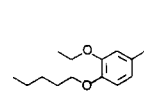			CT 112	Senju, Japan

Figure 2. Clinically tested aldose reductase inhibitors containing hydantoin ring or related ring systems.

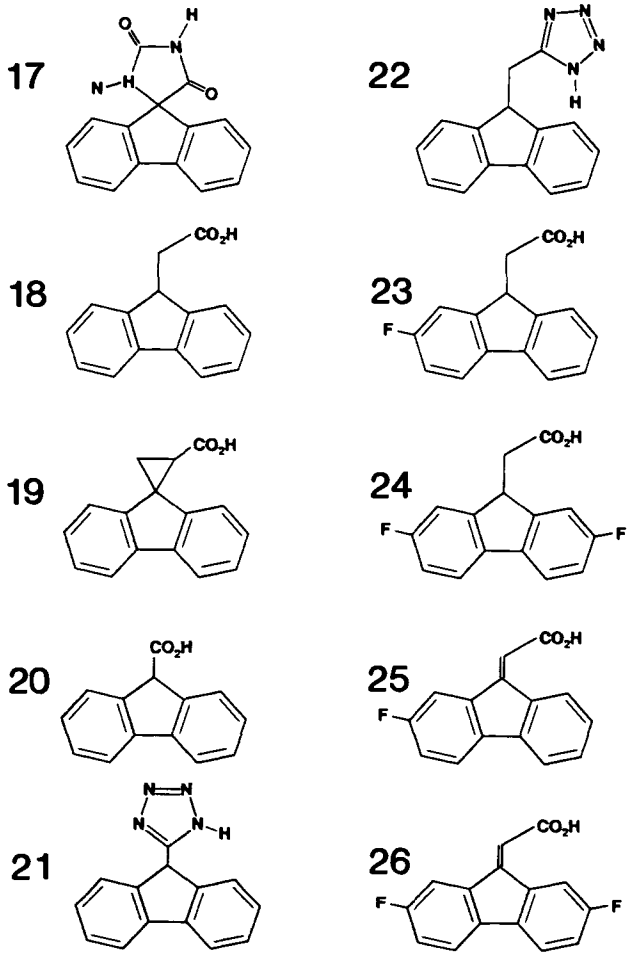

Figure 3. Fluorenecarboxylate and analogues.

an ionizable group and/or functional group susceptible to a nucleophilic attack with the aim of both elucidating the nature of inhibition of the enzyme by ARIs and refining the spatial features of the previously proposed inhibitor site. Quantum chemical calculations have been conducted on compounds **17–26** (Figure 3) which possess an ionizable group, and these optimized structures of compounds **18–26** have been superimposed on **17**. These studies were conducted to determine if a common connection could be established between the activities of these carboxylic acids and the ionizable spirohydantoins. Secondly, calculations have been conducted on the ARIs (**1**, **3**, **5**, **7**, and **8**) which possess both an ionizable group and a functional group. The optimized structures were then superimposed on **17** to define the site at which a reversible charge transfer can occur.

Methodology

Geometry optimization and energetics calculations for compounds (**1**, **3**, **5**, **7**, **8**, and **17–26**) have been conducted at the semiempirical quantum chemical level by utilizing the AM1 Hamiltonian[14] as implemented in MOPAC 6.0.[15] The use of the AM1 Hamiltonian for obtaining the geometries and energetics of small organic molecules has been well documented in the literature.[14] Full geometry optimization with the keywords EF, GNORM=0.01, and MMOK (for compounds containing an amide bond) was performed for all compounds studied. Calculations were conducted on charged (−1) rather than neutral species since the active form of compounds (**1**, **3**, **5**, **7**, **8**, and **17–26**) are assumed to be negatively charged at physiological pH. Evidence for the requirement of a negative charge comes from observations that inhibitory activity is sharply reduced by esterification of certain carboxylic acids containing inhibitors such as alrestatin[3,16] and by the observation that 5′-substituted hydantoins require the ionized form of the hydantoin ring for inhibition.[17]

Superposition of these geometry-optimized compounds was carried out using the torsional flexible fit of Quanta 3.3 (Molecular Simulations, Inc). The torsional flexible fit method minimizes the root mean square (RMS) deviation between two structures as a function of both conformational and orientational degrees of freedom. In this study, the fluorene spirohydantoin **17** was selected as a rigid template onto which all other structures in the series were flexibly fit. The fluorene spirohydantoin **17** was chosen as the template because (1) it contains a rigid hydantoin ring possessing two possible enzyme interaction sites (carbonyl) whose relative position in space is fixed and (2) it has a high affinity for rat lens aldose reductase (RLAR) as indicated by its IC_{50}.

The energy difference (ΔE) between the geometry-optimized and torsionally fitted structure for each working compound was computed to determine whether the torsionally fitted structure is energetically accessible. Energy calculations on the torsionally fitted structures were performed using the keyword 1SCF. ΔE here is defined as the difference in AM1 heat of formation (ΔH_f) between a geometry-optimized and a torsionally fitted conformation.

Results and Discussion

I. Compounds Containing an Ionizable Group. While compounds **18–26** do not possess functional groups susceptible to nucleophilic attack, some of these compounds possess aldose reductase inhibitory activity comparable to that of **17** (see Table 1). Each of these compounds possesses a fused fluorene ring as a common backbone and an ionizable substituent group (carboxylic acid or tetrazole) at the 10-position. Since these compounds share a common backbone, their variance in IC_{50} may well be hypothesized to correlate with the different spatial positions of their ionizable groups attached to the common backbone in their most optimal RMS fit to **17**.

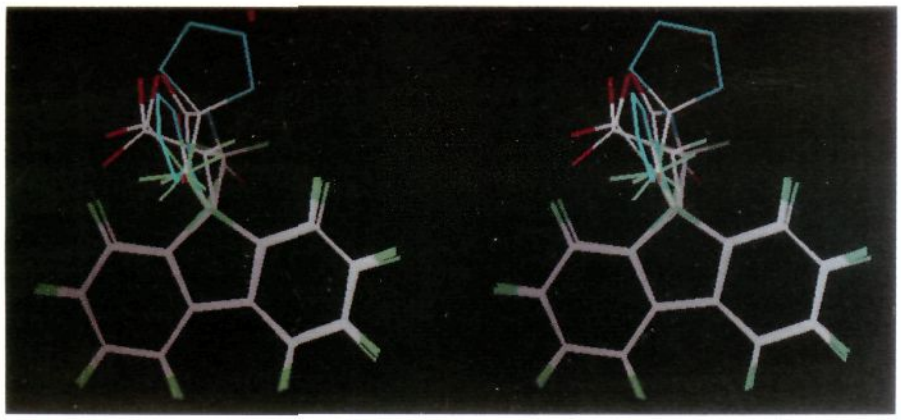

Figure 4. Stereoview of the superimposed structures of 18–22 on 17.

Table 1. Activity of ARIs and Calculated Parameters from the Superimposition of 18–26 on 17

compd	IC_{50} (μM) RLAR[a]	distance (Å) between the charge center d_2	d_4	RMS (Å) r_2	r_4	ΔE (kcal/mol) E_2	E_4
17	3.5						
18	8.9	0.06	0.45	0.02	0.16	0.9	10.4
19	11.7	0.54	1.39	0.19	0.41	4.7	2.8
20	182	1.04	0.35	0.29	0.14	2.3	2.3
21	217	0.91	0.32	0.25	0.11	0.0	0.0
22	1488	0.16	0.61	0.05	0.21	0.3	7.6
23	0.85	0.00	0.52	0.03	0.18	0.9	10.2
24	0.43	0.01	0.53	0.03	0.18	1.0	10.0
25	56	0.37	1.94	0.03	0.62	7.7	0.7
26	16	0.38	1.93	0.13	0.62	8.5	0.8

[a] RLAR (purified rat lens aldose reductase). d, r, and E with subscripts 2 and 4 represent the calculated values from a fit in which a correspondence between an electronegative atom of a working compound and the respective 2′-oxygen atom and 4′-oxygen atom of the hydantoin ring of 17 was made.

To investigate this possibility, compounds 18–26 have been fitted to 17.

Since the fitting requires that corresponding sets of atoms must be assigned to the working and reference molecules, the common fluorene ring of each working and reference compound was chosen. In addition to the fused ring, a correspondence between an electronegative atom (carboxylic oxygen or nitrogen in the tetrazole) of the working compounds and the 2′-oxygen or 4′-oxygen atom of the hydantoin ring of 17 was made to optimize the fit of the negative charge centers. The superimposed structures of compounds (18–22) obtained utilizing the torsional flexible tool of Quanta 3.3 are illustrated in Figure 4.

Figure 4 indicates that the anionic group of each compound is clustered around the 2′-oxygen atom of the hydantoin ring in the best RMS fit of these molecules. From these superposed structures, attempts were made to devise a parameter to represent the trend in the observed activities of compounds 18–22. The distance between the electronegative atom of the negatively charged groups of the working compounds and the 2′-oxygen atom of the hydantoin ring of 17 was one of the choices. This distance parameter gives a qualitative description of how well these negatively charged groups coincide with the 2′-oxygen atom of the hydantoin ring. Compounds 18–22 do not have fluorine atoms, and thus lipophilicity or electron density due to the fluorine atoms is not a factor for giving the different values of IC_{50} for 18–22.

The inhibitory activity of ARIs 17–26 along with the computed distance between charge centers (d_2 and d_4) which correspond to the two different ring superposition orientations aligning each of the carbonyl oxygens of 17 and ΔE all at the least RMS deviation of the optimal fits are summarized in Table 1. A trend between the IC_{50} of the working compounds (18–21) and d_2 was observed with a decreased distance between the charge centers of the working compounds and the 2′-oxygen of the hydantoin ring resulting in higher inhibitory activity. A plot of IC_{50} vs d_2 (Figure 5a) illustrates this trend. The low ΔE (≤4.7 kcal/mol) between the fully AM1 optimized structures in their most stable conformations and the torsionally fitted structures suggest that the conformations of the fitted structures (18–21) are accessible. The superposition orientations of compounds 18–21 with 17, which permit the alignment of the anion of 18–21 and the 4′-oxygen atom of the hydantoin ring, demonstrates no similar trend in IC_{50} vs d_4 (see Figure 5b). It is further noted that the conformation of 18 in Figure 5b is not readily accessible since the fitted conformation of 18 is 10.4 kcal/mol higher in energy than its global minimum.

The inhibitory activity of 18 is ca. 20-fold higher than that of 20. This can be attributed to the fact that d_2 for 18 is shorter than that of 20 by 0.98 Å; however, this trend was not observed for 21 and 22. The IC_{50} of compound 22 is 7-fold lower than that of 21 although d_2 for 22 is shorter by 0.75 Å. Therefore d_2 does not appear to be a good descriptor for describing the inhibitory activity of 22. The tetrazole moiety of 22 occupies a different position in space compared to that of other compounds being located above the 2′-oxygen atom of the hydantoin ring while the anionic groups of the other compounds occupy a position below or adjacent to the 2′-oxygen atom (see Figure 4). Therefore, the tetrazole moiety of 22 may extend into a sterically unallowed region of the active site of aldose reductase (shown above the dotted line in Figure 6). Compounds 20 and 21 have similar activities, and the difference in d_2 for 20 and 21 is only 0.13 Å. Both the carboxylic and tetrazole anions of 20 and 21 span a similar position in space as shown in Figure 4. This suggests that the difference in charge distribution between the carboxylic anion and the tetrazole anion is not a major factor in governing the activity of 20 and 21.

In addition to the distance parameter, conformational energetics and other properties such as lipophilicity and electron density also play important roles in determining the inhibitory activities of 23–26. The differences in activities of compounds 18 versus 23 and 24, and 25 versus

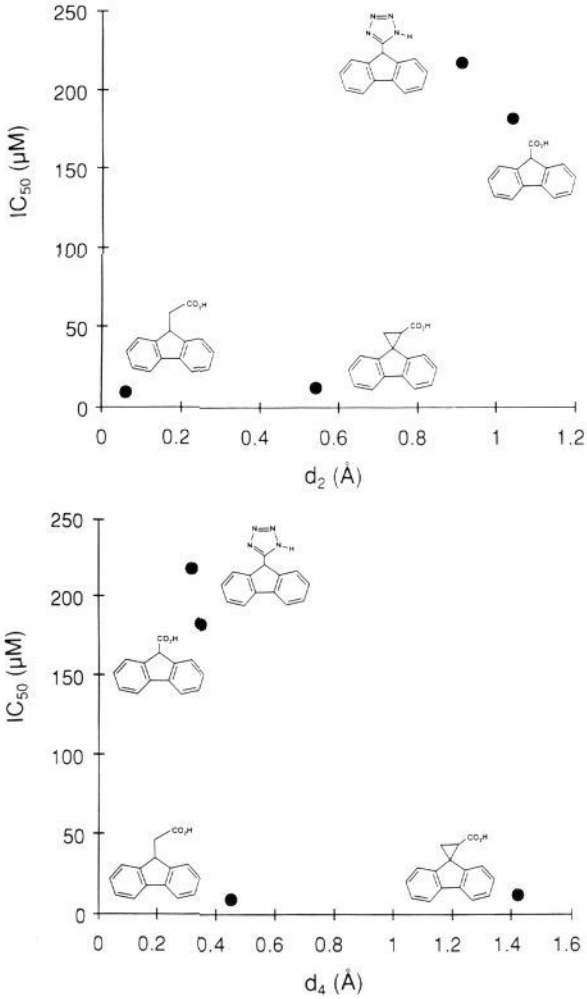

Figure 5. (a) Plot of IC_{50} vs the distance (d_2) between the electronegative atom of the working compounds (**18**–**21**) and the 2′-oxygen atom of the hydantoin ring. (b) Plot of IC_{50} vs the distance (d_4) between the electronegative atom of the working compounds (**18**–**21**) and the 4′-oxygen atom of the hydantoin ring.

26 may be due to an increase in lipophilicity of **18** and **25** or an increased electron density upon the introduction of fluorine. The IC_{50} difference between **23** and **25** can be attributed to the difference in energetics between the two compounds. The difference in d_2 for **23** and **25** is only 0.37 Å; however, **23** is ca. 66-fold more potent than **25**. Energetics associated with the conformation of the carboxylic anion may account for this difference. As summarized in Table 1, the fitted conformation of **25** is 7.7 kcal/mol higher in energy than the minimum conformation whereas the fitted conformation of **23** is only 0.9 kcal/mol higher than its minimum. Therefore, the fitted conformation of **25** from which d_2 (0.37 Å) was calculated is not readily energetically accessible. This suggests that the carboxylic anion of **25** cannot properly orient in the binding site of aldose reductase, and as a result **25** inhibits the enzyme less than compound **23**.

Our finding with regard to the required location of the negative charge site is in agreement with those of Yamagashi et al.[13] who have investigated the importance of the hydantoin ring in ARI activity by modifying the hydantoin ring of **27** and concluded that the modified hydantoins **29**–**31** were much less potent than **28**. Compounds **29**–**31** all lack the 2′-oxygen atom of the hydantoin ring, which

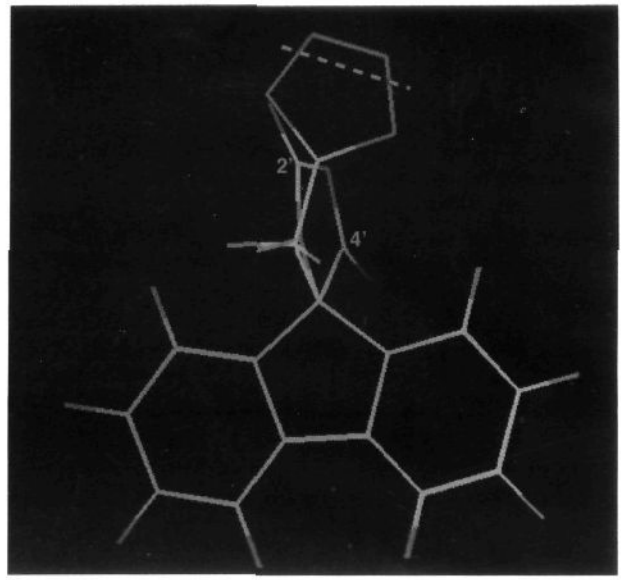

Figure 6. Superimposed structure of **22** on **17**.

the present study identifies as an important negative charge center influencing the activity of ARIs.

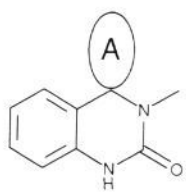

27

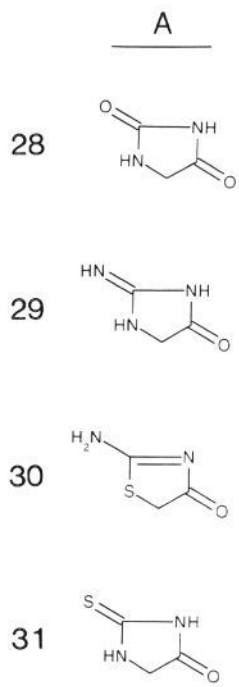

II. Compounds Containing both an Ionizable Group and a Carbonyl or Thione. Compounds summarized in Figure 1 containing both an ionizable group and an additional carbonyl or thione (C=S) that can undergo nucleophilic attack were investigated to pinpoint the site of nucleophilic substitution. Experimental evidence for nucleophilic substitution comes from observations of the existence of nucleophilic residue, in or near the inhibitor binding site,[5] and from the use of affinity labels derived from **17**, alrestatin (**1**), and sorbinil (**9**). The 4′-carbonyl of **17** is the most probable site of nucleophilic attack based on evidence that the reactivity of the 4′-carbonyl to attack by base is increased with the ionization of the 3′-position imide in 5′-substituted hydantoins.[18]

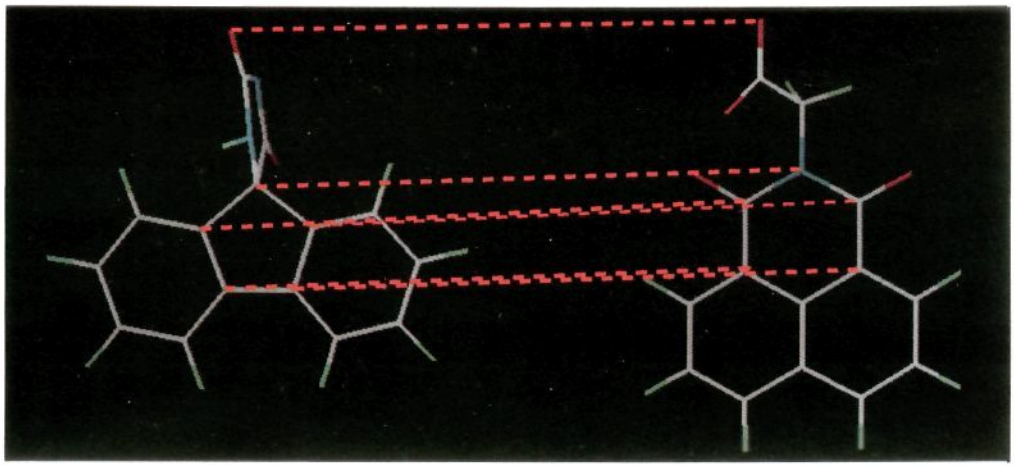

Figure 7. Equivalent sets of atoms for working and reference compounds.

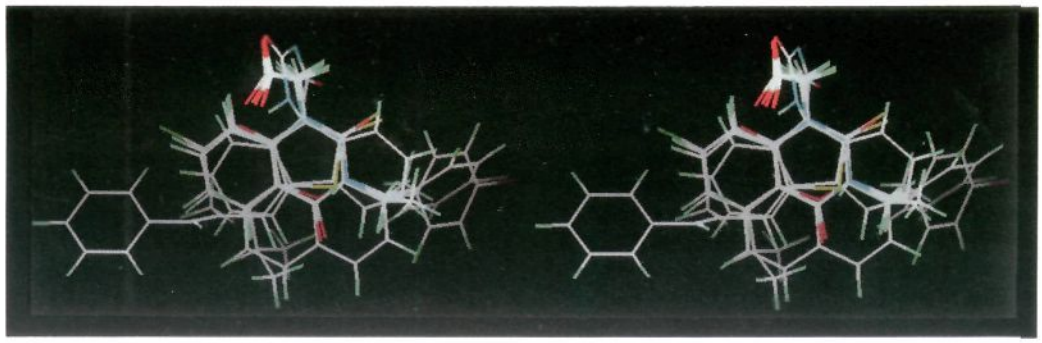

Figure 8. Stereoview of the superimposed structure of 1, 3, 5, 7, and 8 on 17.

Compounds 1, 3, 5, 7, and 8 were superimposed on 17 to pinpoint the site at which nucleophilic substitution occurs.

Since compounds 1, 3, 5, 7, and 8 do not have a fluorene ring as a common backbone, there is no unique way, with the exception of the carboxylic anion, of superimposing these compounds on 17. Superimposition of compounds 1, 3, 5, 7, and 8 on 17 was performed by choosing the corresponding atoms illustrated in Figure 7, where a set of five ring atoms and an oxygen atom of the carboxylic anion of 1, 3, 5, 7, and 8 correspond to the set of five atoms and the 2′-oxygen atom of the hydantoin ring. This allowed low-energy conformations of 1, 3, 5, 7, and 8 to be well fitted to 17. The two torsional angles shown in 32 were allowed to vary for each compound during torsional flexible fitting to 17. Other rotatable bonds in 3, 5, 7, and 8 were frozen in a minimum-energy conformation.

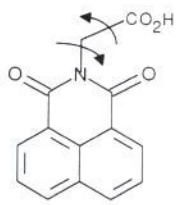

32

Figure 8, depicting the superimposed structures 1, 3, 5, 7, and 8 on 17, illustrates that the carboxylic anion of the working compounds fits well to the 2′-oxygen atom of the hydantoin ring. It also shows that the hydrophobic portion (aromatic ring) of the working compounds overlaps well

Table 2. Activity of ARIs and Calculated Parameters from the Superimposition of 1, 3, 5, 7, and 8 on 17

compd	IC_{50} (μM) RLAR	distance (Å) d_2	RMS (Å) r_2	ΔE (kcal/mol) E_2
1	1.5[a]	0.21	0.37	2.5
3	0.016[a]	0.07	0.31	2.8
5	0.0044[b]	0.13	0.26	1.6
7	0.023[c]	0.19	0.24	0.2
8	0.13[c]	0.11	0.31	1.6

[a] *Reference 19.* [b] *Reference 20.* [c] *Reference 21.*

that of 17. From this superposition, the d_2, RMS, and ΔE between the unfitted and the torsionally fitted structures have been calculated. The activities of ARIs and the calculated parameters from the fitting are listed in Table 2. Values for d_2 for compounds 1, 3, 5, 7, and 8 range from 0.07 to 0.21 Å, indicating that the spatial positions of the carboxylic anion of these working compounds are very close to the 2′-oxygen of the hydantoin ring. The torsionally fitted structures of 1, 3, 5, 7, and 8 are all energetically accessible since ΔE is ≤2.8 kcal/mol. Since compounds 3, 5, 7, and 8 have a number of rotatable bonds, extensive conformational studies to differentiate the global minimum of each working compound were not conducted. Therefore in Table 2 ΔE reflects the difference between the energy of a stable conformer of the working compounds and the energy of their respective torsionally fitted structure.

A diagram (Figure 9) estimating the region at which nucleophilic charge transfer is likely to take place was constructed by taking the spatial position of carbonyl or thiocarbonyl of 1, 3, 5, 7, and 8 with respect to the 4′-carbonyl of the hydantoin ring from Figure 8. Figure 9 illustrates that positions of C_1 and C_2 are in close proximity

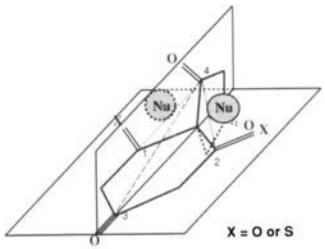

Figure 9. Spatial regions where nucleophilic substitution is likely taking place.

to the 4′-carbonyl carbon atom (C_4) of the hydantoin ring whereas position C_3 is relatively distant. Since nucleophilic substitution is likely to occur at the 4′-carbonyl of the hydantoin ring, the position C_3 can be excluded from the region where nucleophilic substitution taking place. The nucleophile (Nu) may reside at a position between the 4′-carbonyl of the hydantoin ring and C_1 or C_2 as shown in Figure 9. The mapping of the spatial position of a proposed nucleophilic residue of aldose reductase will be published elsewhere. On the basis of Figure 9, it can be postulated that the inhibitory activity of **3** is primarily governed by the presence of the carboxylic anion but not by the carbonyl, while the activity of **1**, **5**, **7**, and **8** is dictated by both the carboxylic anion and carbonyl or thiocarbonyl. The carbonyl or thiocarbonyl of **1**, **5**, **7**, and **8** is susceptible to nucleophilic attack since it spans a region close to the 4′-carbonyl of the hydantoin ring.

Summary

A connection has been established between the activities of two major structural classes of ARIs by demonstrating that a negative charge center residing in the vicinity of the 2′-oxygen atom of the hydantoin ring participates in binding interactions. The distance parameter, d_2, together with conformational energetics and excluded steric volume, appears to be a good descriptor for explaining the difference in the observed activities of ARIs **18**–**26**. Compounds **1**, **3**, **5**, **7**, and **8** containing both an ionizable group and a functional group help to define the region where reversible charge transfer most likely takes place. Understanding the pharmacophore requirements may lead to the rational design of new ARIs.

References

(1) Kador, P. F. The Role of Aldose Reductase in the Development of Diabetic Complications. *Med. Res. Rev.* **1988**, *8*, 325.
(2) Kador, P. F.; Akagi, Y.; Terubayashi, H.; Wyman, M.; Kinoshita, J. H. Prevention of Pericyte Ghosts in Retinal Capillaries of Galactose-fed Dogs by Aldose Reductase Inhibitors. *Arch. Ophthalmol.* **1988**, *106*, 1109.
(3) Kador, P. F.; Nakayama, T.; Sato, S.; Smar, M.; Miller, D. What is the Nature of the Charge Transfer Interaction at the Aldose Reductase Inhibitor Site? *Prog. Clin. Biol. Res.* **1989**, *292*, 237.
(4) Kador, P. F.; Sharpless, N. E. Structure-activity studies of Aldose Reductase Inhibitors Containing the 4-oxo-4*H*-chromen ring system. *Biophys. Chem.* **1978**, *8*, 81.
(5) Kador, P. F.; Sharpless, N. E. Pharmacophor Requirements of the Aldose Reductase Inhibitor Site. *Mol. Pharmacol.* **1983**, *24*, 521.
(6) Kador, P. F.; Sharpless, N. E.; Kinoshita, J. E. A Potent New Class of Agents for the Pharmacological Control of Certain Diabetic Complications. *J. Med. Chem.* **1985**, *28*, 841.
(7) Ares, J. J.; Kador, P. F.; Miller, D. D. Synthesis and Biological Evaluation of Irreversible Inhibitors of aldose reductase. *J. Med. Chem.* **1986**, *29*, 3834.
(8) Kador, P. F.; Gurley, R. C.; Ares, J. J.; Miller, D. D. Irreversible Aldose Reductase Inhibitors. *Prog. Clin. Biol. Res.* **1987**, *232*, 353.
(9) Smar, M. W.; Ares, J. J.; Nakayama, T.; Itabe, H.; Kador, P. F.; Miller, D. D. Selective Irreversible Inhibitors of Aldose Reductase. *J. Med. Chem.* **1992**, *35*, 1117.
(10) DeRuiter, J.; Brubaker, A. N.; Whitmer, W. L.; Stein, J. L. Synthesis and Aldose Reductase Inhibitory Activity of Substituted 2-Oxoquinone-1-acetic Acid Derivative. *J. Med. Chem.* **1986**, *29*, 2024.
(11) Ellingboe, J.; Alessi, T.; Millen, J.; Sredy, J.; King, A.; Prusiewicz, C.; Guzzo, F.; VanEngen, D.; Bagli, J. (Pyrimidinyloxy)acetic Acids and Pyrimidineacetic Acids as a Novel Class of Aldose Reductase Inhibitors. *J. Med. Chem.* **1990**, *33*, 2892.
(12) Malamas, M. S.; Millen, J. Quinazolineacetic Acids and Related Analogues as Aldose Reductase Inhibitors. *J. Med. Chem.* **1991**, *34*, 1492.
(13) Yamagishi, M.; Yamada, Y.; Ozaki, K.; Assao, M.; Shimizu, R.; Suzuki, M.; Matsuoko, Y.; Matsumoto, K. Biological Activities and Quantitative Structure-Activity Relationships of Spiro(imidazoline-4,4′(1′*H*-quinazoline]-2,2′,5(3′*H*)-triones as Aldose Reductase Inhibitors. *J. Med. Chem.* **1992**, *35*, 2085.
(14) Dewar, M. J. S.; Zoebisch, E. G.; Healy, E. F.; Stewart, J. J. P. A New General Purpose Quantum Mechanical Molecular Model. *J. Am. Chem. Soc.* **1985**, *107*, 302.
(15) Stewart, J. J. P. *QCPE Bull.* **1990**, 455, MOPAC Version 6.0.
(16) Dvornik, D. In Aldose Reductase Inhibition. An Approach to the Prevention of Diabetic Complications. Biomedical Information Corporation; Porte, D., Ed.; McGraw-Hill: New York, 1987; Chapter 4.
(17) Inagaki, K.; Miwa, I.; Yashiro, T.; Okuda, J. Inhibition of Aldose Reductase from rat and bovine lenses by hydantoin derivatives. *Chem. Pharm. Bull.* **1982**, *30*, 3244.
(18) Aspeuland, H.; Waselund, H.; Waselius, P. Resistance of Hydantoins and 5-Hydroxyhydantoins to Alkali. *Acta Acad. Abo. Math. Phys.* **1967**, *27*, 1.
(19) Sato, S.; Kador, P. F. Inhibition of Aldehyde Reductase by Aldose Reductase Inhibitors. *Biochem. Pharmmacol.* **1990**, *40*, 1033.
(20) Ao, S.; Shingu, Y.; Notsu, Y.; Kikuchi, C.; Yamaguchi, I. In *Characterization of a Novel Aldose Reductase Inhibitor, FR-74366: Current Concepts of Aldose Reductase and its Inhibition*; Sakamoto, N. Kinoshita, J. H., Kador, P. F., Hotta, N., Eds.; Elsevier Science: Amsterdam, 1990; pp 81–88.
(21) Ikeda, H. In *Pharmacological Profile of AD-5467, A New Aldose Reductase Inhibitor: Current Concepts of Aldose Reductase and Its Inhibitions*; Sakamoto, N., Kinoshita, J. H., Kador, P. F., Hotta, N., Eds.; Elsevier Science: Amsterdam, 1990; pp 97–103.